Available online at www.sciencedirect.com

ScienceDirect

Physics Procedia 61 (2015) 719 – 723

Physics Procedia

13th International Conference on Topics in Astroparticle and Underground Physics, TAUP 2013

Understanding the SNO+ Detector

K. Kamdin* , for the SNO+ Collaboration

Lawrence Berkeley National Laboratory, 1 Cyclotron Road Mail Stop 50R5008, Berkeley, CA 94720, USA

University of California, Berkeley, 366 LeConte Hall #7300 Berkeley, CA 94720-7300, USA

Abstract

SNO+, a large liquid scintillator experiment, is the successor of the Sudbury Neutrino Observatory (SNO) experiment. The scintillator volume will be loaded with large quantities of ^{130}Te, an isotope that undergoes double beta decay, in order to search for neutrinoless double beta decay. In addition to this search, SNO+ has a broad physics program due to its sensitivity to solar and supernova neutrinos, as well as reactor and geo anti-neutrinos. SNO+ can also place competitive limits on certain modes of invisible nucleon decay during its first phase.

The detector is currently undergoing commissioning in preparation for its first phase, in which the detector is filled with ultra pure water. This will be followed by a pure scintillator phase, and then a Tellurium-loaded scintillator phase to search for neutrinoless double beta decay.

Here we present the work done to model detector aging, which was first observed during SNO. The aging was found to reduce the optical response of the detector. We also describe early results from electronics calibration of SNO+.

Selection and peer review is the responsibility of the Conference lead organizers, Frank Avignone, University of South Carolina, and Wick Haxton, University of California, Berkeley, and Lawrence Berkeley Laboratory

Keywords: neutrino; neutrinoless double beta decay; liquid scintillator; Tellurium

---

1. The SNO+ Experiment

The SNO+ experiment reuses the existing Sudbury Neutrino Observatory (SNO) detector, located at a depth of 6000 meters water equivalent in SNOLAB. At the heart of the detector is a 12m diameter acrylic vessel, which held heavy water during SNO and will hold the Tellurium-loaded liquid scintillator during the neutrinoless double beta decay search in SNO+ (see Figure 1 and Boger et al. (2000) for more details on SNO). The scintillator target allows for a low energy threshold on the order of 1MeV. When charged particles pass through the scintillator, the emitted

---

* Corresponding author.
E-mail address: kkamdin@berkeley.edu

Selection and peer review is the responsibility of the Conference lead organizers, Frank Avignone, University of South Carolina, and Wick Haxton, University of California, Berkeley, and Lawrence Berkeley Laboratory
doi:10.1016/j.phpro.2014.12.087

light is detected by ~9,500 photomultiplier tubes (PMTs) that view the acrylic vessel. The energy and position of each event are reconstructed from the PMT signals.

The SNO+ scintillator will consist of linear alkyl benzene (LAB) and 2g/L of the fluor 2-5 diphenyloxazole (PPO). LAB is chemically compatible with acrylic, non-toxic, has good optical transparency, low scattering, and fast decay time.

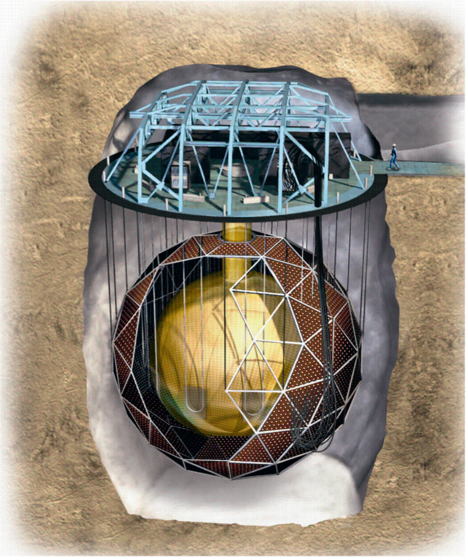

Figure 1: The SNO+ detector consists of a 12 meter diameter acrylic sphere containing the active volume. A 54 % optical coverage is given by ~9500 PMTs placed in a 17 meter diameter geodesic structure, with interior and exterior shielding by pure water.

In addition to the scintillator target, SNO+ has other modifications from SNO. A new rope system has been installed to hold down the scintillator-filled acrylic vessel, which is now buoyant in the light-water shield. New scintillator purification systems have been designed to reach the required U and Th contamination levels (Ford et al. (2010)). Lastly, a new system for inserting calibration sources has been designed, and the data acquisition electronics have been upgraded to handle the higher data rates.

2. Neutrinoless Double Beta Decay with SNO+

Double beta decay ($2\nu\beta\beta$) is a rare process that occurs naturally in a few isotopes. If neutrinos are Majorana particles, another possible decay mode exists where the two electrons carry the full energy difference between the mother and daughter nuclei (Q), and no neutrinos are emitted ("neutrinoless double beta decay" or $0\nu\beta\beta$). The rate of $0\nu\beta\beta$ decay depends on an effective neutrino mass, mass-mixing parameters, and Majorana phases. Thereby, $0\nu\beta\beta$ is a probe of the absolute neutrino mass scale as well as the neutrino hierarchy. The decay rate would also depend, differently for each isotope, on phase space parameters and nuclear matrix elements governing the decay.

SNO+ will look for neutrinoless double beta decay in ^{130}Te, which has a Q-value of 2.53 MeV. The loading technique developed for the $0\nu\beta\beta$ search involves dissolving telluric acid in water, and adding this mixture to the LAB-PPO mix using a surfactant. The resulting scintillation cocktail does not exhibit any strong absorption lines in the range where the SNO+ PMTs are most sensitive. It is possible to load ^{130}Te in high concentrations without affecting the optical clarity of the scintillation mixture; future loading of 3% natural Te is being investigated as a successor to the planned 0.3% natural Te phase of SNO+. The 0.3% Te phase is expected to reach sensitivities to Majorana neutrino masses approaching the top of the inverted neutrino mass hierarchy. For more information on SNO+ with Tellurium, see Biller (2014).

3. Concentrator Aging

Each of the SNO+ PMTs is surrounded by a reflective, light-enhancing cone called a concentrator (see Figure 2 (a)). During the SNO experiment, the concentrators were observed to degrade, which in turn decreased the response of the detector to light. SNO+, as SNO, uses the so-called "angular response" to characterize the response of the PMT and concentrator combination to light as a function of incident angle (see Figure 2 (b)). Angular response is the fraction of incident photons that cause a successful PMT hit, binned at each angle relative to the PMT normal; it is wavelength dependent. Properly modeling any detector components that affect angular response is essential for accurate event reconstruction, particularly the position dependence of energy reconstruction.

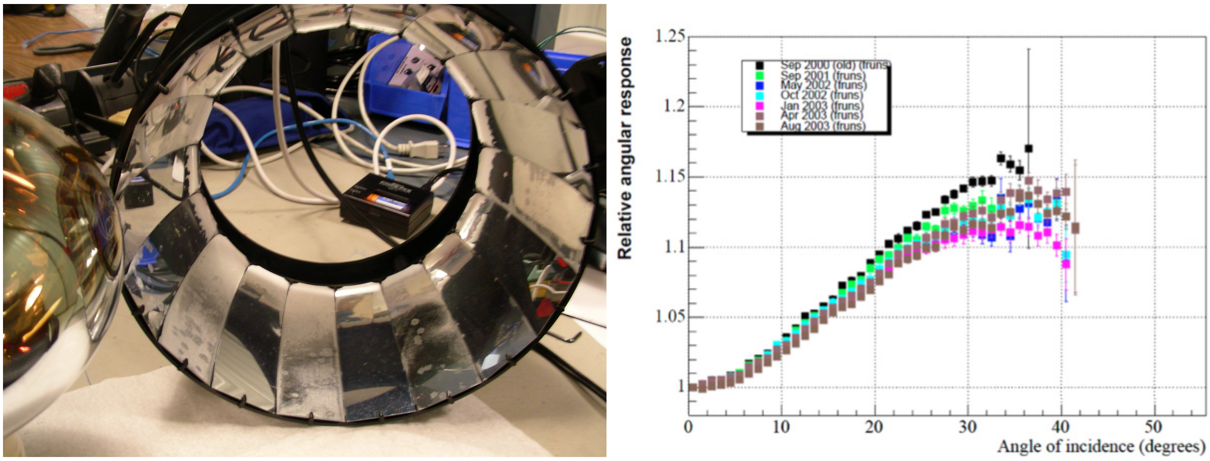

(a) (b)

Figure 2: The concentrator (a) surrounds each PMT to increase light-collection. A degraded concentrator reduces light collection, and thereby the ability to accurately reconstruct event energies. The angular response (b), used to characterize the response of the PMT and concentrator combination to light as a function of incident angle, was seen to decrease at high angles over the course of the SNO experiment.

An aging model and fitting routine have been developed to model concentrator aging in SNO+. The basic aging model is an increase in diffuse reflectivity and absorption, with a corresponding decrease in specular reflectivity, in the SNO+ Monte Carlo model (RAT) of the concentrators. The changes to these reflectivities can be dependent on the position the incoming photon strikes the concentrator to mimic the non-uniform aging observed on the concentrators. The parameters that describe the position dependence and overall magnitude of the change to the default reflectivities are referred to as "aging parameters."

The fitting method uses a class called MiniSim, which is a simplified version RAT, and the ROOT TMinuit class to perform a χ^2 minimization. With each iteration of the fit, MiniSim runs with different aging parameters and produces an angular response. The MiniSim angular response is then compared to the "data" we are fitting via χ^2. The "data" is a RAT simulation with known aging parameters (for testing) or SNO data.

The fitting routine converges quickly and accurately for a simple test case, and the full fitting routine is under development.

4. Electronic Calibration

The electronic calibration (ECA) is the first step in turning raw data into meaningful physics information. Each SNO+ PMT corresponds to an electronic channel with 16 12-bit ADC cells that temporarily store information until the detector triggers. Each cell stores several values that will later be converted into charges (called QHS, QHL, and QLX) and hit times. The ECA analysis calculates the pedestal values for the three measured charge values. The pedestal values are the zero charge values (in ADC counts) that the channel returns when there is no actual PMT hit.

The ECA analysis also calculates the slope of the time-to-amplitude converter (TAC slope). When a PMT registers a hit, the TAC voltage starts to ramp. Calculating the slope of this ramp allows for the conversion of ADC counts into time (ns).

Unstable or invalid ECA constants are the first sign that a channel is malfunctioning. Channels that have consistently bad ECA values or have ECA values that vary wildly from calibration to calibration can be tagged as malfunctioning and removed from physics data taking.

ECA pedestal values from dry commissioning runs in SNO+ were compared to SNO pedestal values to get an impression of the stability of the PMTs. This is important, as the PMTs in the SNO+ detector are mostly the same PMTs as were used in SNO. The distributions of several pedestal-type ECA calibration runs from SNO match with those of SNO+ , illustrating that, on the average, the SNO+ channels are behaving as expected (Figure 3 (a)). As a test of the analysis software, ECA data from SNO was analyzed with RAT and the results were compared to the results from the SNO data analysis software, SNOMAN, in order to ensure that RAT extracts the same constants as SNOMAN. The results of the software comparison were also very favorable: the SNOMAN results were essentially identical to the RAT results in a cell-by-cell comparison. Figure 3 (b) shows SNOMAN results subtracted cell-by-cell from RAT results for one ECA run, illustrating that the difference between the two analysis software is well within acceptable limits.

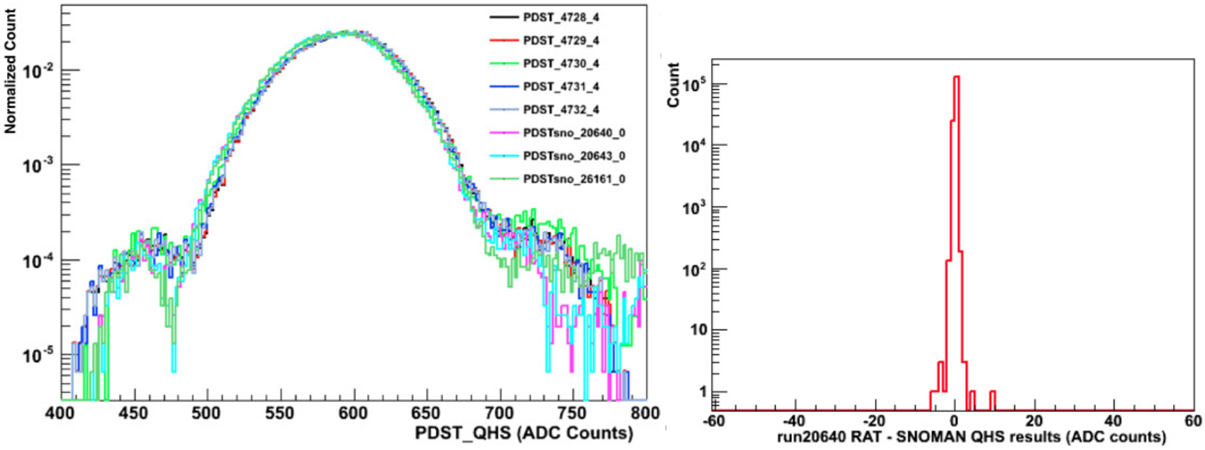

(a) (b)

Figure 3: Several pedestal runs from SNO compared with dry commissioning SNO+ pedestal runs (a). The overlapped distributions confirm that the shapes are the same and that the average pedestal from SNO matches the average pedestal from SNO+. The plots labelled "PDSTsno_XXXXX_X" are SNO data, the others are from SNO+. The results of SNOMAN-analyzed pedestal data subtracted from RAT-analyzed pedestal data show that the two analyses extract nearly the same cell-by-cell constants (b).

5. Conclusions

The SNO+ detector consists of ~9,500 PMTs observing an acrylic vessel that will first contain water, then pure scintillator, and finally scintillator loaded with ^{130}Te. Each PMT corresponds to a channel with 16 ADC cells, and each cell must be calibrated individually. First results from calibration data show that the channels have similar calibration constants as in SNO and that the RAT analysis code is correctly extracting constants.

The SNO+ collaboration will investigate neutrinoless double beta decay with ^{130}Te by initially loading 0.3% natural Te in scintillator. Loading studies show that the scintillator cocktail can accommodate percent-levels of Te without detriment to optical clarity. The $0\nu\beta\beta$ phase in particular requires accurate energy reconstruction. In order to best reconstruct energies and understand the position dependence of energy reconstruction, the aging of the PMT and concentrator combination is being modeled and studied further.

The SNO+ physics targets include a search for neutrinoless double beta decay, low energy solar neutrinos, geo-neutrinos, reactor neutrinos (for the study of Δm^2_{12}), supernova neutrinos, and the search for invisible modes of nucleon decay (which will actually take place during the initial water-fill phase before the transition to scintillator). The detector is currently undergoing commissioning in preparation for water-fill.

References

Biller, S., 2014. SNO+ with Tellurium. (these proceedings).
Boger et al., J., 2000. The Sudbury Neutrino Observatory. Nuclear Instruments and Methods in Physics Research A 449, 172–207.
Ford et al., R., 2010. SNO+ scintillator purification and assay. AIP Conference Proceedings 1338, 183–194.